Indoor Position Estimation using NLoS Information by Wireless Distance Sensors

Tomoya Itsuka[1] and Ryo Kurazume[2]

Abstract— **This paper proposes a method for non-line-of-sight (NLoS) position estimation utilizing wireless distance sensors. Recently, the accuracy of wireless distance sensors that use ultra-wideband (UWB) or ultrasonic technologies to measure the distance between two sensor devices has increased significantly. By placing these sensors in the environment, it is possible to precisely determine the position of mobile robots in indoor environments. Owing to reflections in the environment, these sensors have a large measurement error in NLoS conditions, limiting their applicability to environments that satisfy the line-of-sight (LoS) condition. This study aims to develop a stable method for estimating the position of mobile robots in indoor environments, including NLoS conditions, using wireless distance sensors. Experiments were conducted in two real environments: one with obstacles in front of the beacon and one with dynamic obstacles. In both cases, the combining 2D-LiDAR and wireless distance sensors using the proposed method considering NLOS was more accurate than the method considering LoS only.**

I. INTRODUCTION

Autonomous robot navigation requires a reliable position-estimation method. The GPS can provide a highly accurate location on a map in outdoor environments. However, GPS signals cannot be acquired indoors owing to obstructions created by roofs and walls.

One of the most popular position estimation methods for indoor robots is the adaptive Monte Carlo localization (AMCL) method, which compares the surrounding geometry obtained from a 2D-LiDAR to a pre-constructed occupied grid map. However, reliable location estimation becomes challenging in environments with numerous simple or complex shapes or shapes with similar characteristics. Additionally, the estimation may fail because of the inconsistencies between the map and the actual environment, such as those occurring due to the movement of objects or the modification of floor plans. Furthermore, it is difficult to return to the correct position once the robot's position has been incorrectly estimated.

Recently, the accuracy of wireless distance sensors that use ultra-wideband (UWB) or ultrasonic technologies to measure the distance between two sensor devices has increased significantly. By placing these sensors in the environment, it is possible to precisely determine the position of mobile robots in indoor environments.

[1]Tomoya Itsuka is with Graduate School of Information Science and Electrical Engineering, Kyushu University, Japan. itsuka@irvs.ait.kyushu-u.ac.jp

[2]Ryo Kurazume is with Faculty of Information Science and Electrical Engineering, Kyushu University, Japan. kurazume@ait.kyushu-u.ac.jp

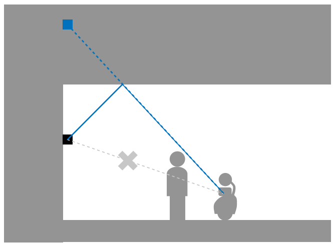

Fig. 1: **Use of ceiling reflection.** If there is an obstacle between the two beacons to be measured, the reflection path is mainly measured. In addition to the real coordinates, the estimation uses the coordinates of the beacon specularly reflected from the ceiling.

However, these sensors have a large measurement error in NLoS (non-line-of-sight) condition due to reflections in the environment, and thus the applicable environments are limited which satisfies the LoS (line-of-sight) condition.

In this study, we propose a position estimation method using wireless distance sensors that also considers the NLoS condition. In the NLoS condition, wireless distance sensors observe a large measurement error owing to reflections in the environment. However, by considering the possible reflection path and combining it with the AMCL method, precise position estimation becomes possible even in NLoS conditions. This paper presents the proposed method and experimental results obtained using ultrasonic sensors in complex environments.

II. RELATED WORK

In the context of simultaneous localization and mapping (SLAM), robot pose estimation by combining 2D-LiDAR and beacons is being investigated, particularly in featureless tunnel and corridor environments where experiments have been conducted [1][2].

Beacon-based methods are subject to errors due to signal reflection and transmission when there are obstacles between the measurement beacons (i.e., NLoS). Previous research has addressed the identification and mitigation of NLoS conditions [3]. Also, studies have been conducted on the use of reflective paths due to interior walls [4][5]. These methods also model the reflection path by considering a virtual beacon as shown in Fig. 1.

In [4], position estimation with a single ultrasonic beacon is proposed by capturing delayed waveform peaks due to reflections as well as the direct path of ultrasonic waves. However, the first peak must be caused by a direct path and this method cannot be applied to environments where direct waves do not reach. In [5], the position estimation using Time Difference of Arrival (TDoA) by three or more beacons in NLoS condition is proposed. However, identifying whether the measured distance is due to direct or reflected paths is time-consuming beacause all combinations of real and virtual beacons must be examined.

This research aims to develop a position estimation method for indoor robots utilizing reflected wave paths, allowing the robot to operate in a stable manner even when NLoS is caused by dynamic obstacles, such as pedestrians.

We utilize a Time of Arrival(ToA)-based ultrasonic beacon as the wireless distance sensor and a particle filter for a position estimation. Each particle identifies whether the measured distance is caused by a direct or reflected path. Therefore, the proposed method can be applied from a single beacon and can be easily added to environments where estimation using LiDAR is difficult.

III. HARDWARE

In this study, an ultrasonic beacon [6] manufactured by Marvelmind, Inc., was used as a wireless distance sensor to determine the distance from a known environmental point. This ultrasonic beacon includes a beacon body capable of transmitting and receiving ultrasonic waves as well as a modem to control multiple beacons. The beacon is comprised of eight different beacons with varying transmission frequencies. Additionally, regardless of the beacon type, all beacons can receive ultrasonic waves with varying frequencies.

Furthermore, we experimented with an inverse architecture (IA) setup[6] where ultrasonic waves were transmitted from a beacon placed in the environment and received by a beacon mounted on the robot.

IV. MEASUREMENT ACCURACY IN LOS/NLOS CONDITIONS

Experiments were conducted in a room with walls on all four sides and obstacles between beacons to verify the accuracy of the measurement distance under LoS and NLoS conditions. The dimensions of the room were approximately $9m \times 9m$ and the ceiling height $h_c = 3.49[m]$. The transmitting frequencies were $f_{TX} = 31kHz$ and $45kHz$. The transmitting beacon was mounted on the wall at a height of $h_{TX} = 1.8m$ from the floor, while the receiving beacon was placed at a height of $h_{RX} = 0.7m$. The obstacles were wooden walls (desks) with a height of $h_O = 1.82m$.

We measured the distance between the transmitting and receiving beacons when the receiving beacon was placed 1–8 m (1 m increments), away from the wall under three conditions: ① no obstacle (LoS), ② obstacle at $x = 1.0m$ from the transmitting beacon (NLoS-1m), and ③ obstacle at $x = 2.0m$ from the transmitting beacon (NLoS-2m). For each condition, the distance was measured 1000 times, and the average distance was calculated.

The results are shown as box plots and scatter plots in Fig. 3. For $x = 1.0m$ in the NLoS-1m condition and $x = 2.0m$ in the NLoS-2m condition, measurements were taken as close to the desk as possible. The theoretical values of the direct

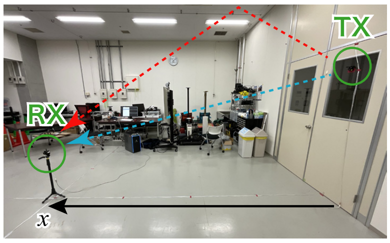

(a) LoS. Blue arrows represent the distance in a straight line, while red arrows represent the path for reflection by the ceiling.

(b) NLoS-1m

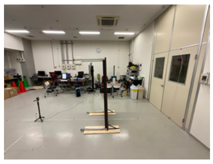

(c) NLoS-2m

Fig. 2: Experimental setup

distance d^* and reflection distance from the ceiling $d^{r,*}$ are also plotted.

$$\begin{aligned} d^* &= |\boldsymbol{x}_{RX} - \boldsymbol{x}_{TX}| \\ &= \left| \begin{pmatrix} x \\ 0 \\ h_{RX} \end{pmatrix} - \begin{pmatrix} 0 \\ 0 \\ h_{TX} \end{pmatrix} \right| \end{aligned} \tag{1}$$

$$d^{r,*} = \left| \begin{pmatrix} x \\ 0 \\ h_{RX} \end{pmatrix} - \begin{pmatrix} 0 \\ 0 \\ h_c + (h_c - h_{TX}) \end{pmatrix} \right| \tag{2}$$

As a result, the direct distance between beacons can be measured with high accuracy in an environment with no obstacles (LoS). In an environment with obstacles (NLoS-1m, NLoS-2m), the measured distance is greater and closer to the ceiling reflection path than in the absence of obstacles.

In environments where the beacon is in contact with an obstacle, such as during the 1-meter measurement at NLoS-1m and the 2-meter measurement at NLoS-2m, the reflection path from the ceiling is also blocked, resulting in sparse measurements.

V. PROPOSED METHOD

The proposed method aims to achieve stable and precise indoor position estimation by incorporating the likelihood from wireless distance sensors under NLoS conditions into the AMCL, which is widely used for indoor mobile robots.

A. Adaptive Monte-Carlo localization

AMCL [7] is a particle filter-based localization method. The particle filter maintains a set of candidate points as a set of particles and estimates position by repeating the steps below:

- Prediction Step
  Consider the odometry as a control signal u_t, and move each particle by sampling from the motion model $p(x_t|u_t, x_{t-1})$.
- Observation Step

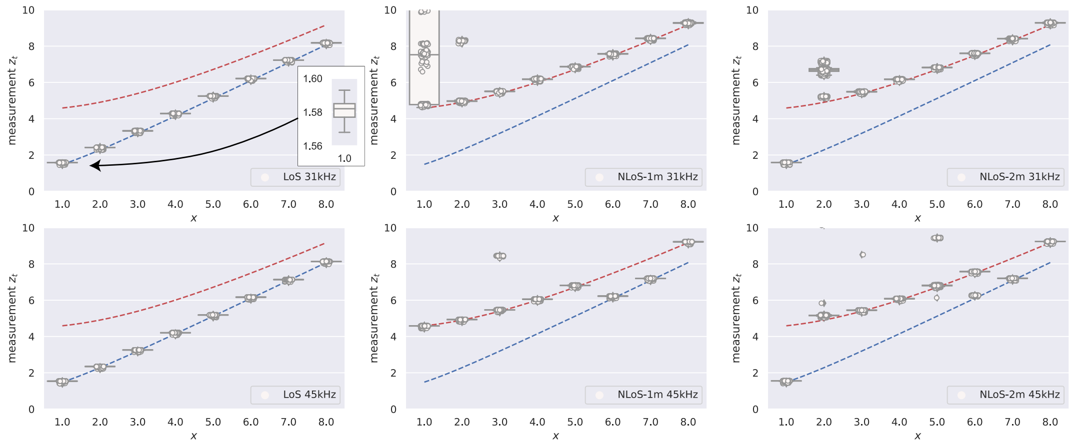

Fig. 3: **Measurement Experimental Results.** Box-and-whisker and scatter plots are depicted. The horizontal axis is the horizontal distance between receiving and transmitting beacons $[m]$, and vertical axis is the measured value $[m]$. The blue and red dotted lines are the theoretical values of the direct and ceiling reflection paths, respectively. The measured distances considerably coincide in most conditions, and the box-and-whisker diagram is collapsed into a horizontal line.

The measurement model $p(z_t|x_t, m)$ is used to calculate the likelihood from the sensor signal, and each particle is weighted.
The likelihood field model [7] is used in this study to match the 2D-LiDAR and the environmental map.

- Resampling Step
  New particles are distributed from the distribution of weighted particles.

In this study, we add an observation step for the integration of beacons using navigation2-amcl[8], a well-known implementation of the AMCL. For simplicity, random particle injection and KLD sampling were not performed, and the number of particles was kept constant.

B. Add likelihood based on beacon distance information

A measurement model was added in order to use the distance measured by the beacon for the observation step described in the previous section. The likelihood based on beacon distance information was implemented using the beam model [7].

- Distribution by measurement error
  First, the ideal measurement distance z^* is calculated from the particle positions and beacon coordinates on the map. The measurement noise is simulated by assuming a normal distribution with standard deviation σ^2_{hit}, centered on z^*.

$$p_{hit}(z_t|x_t, m) = \mathcal{N}(z_t; z^*_t, \sigma^2_{hit}) \tag{3}$$

- Distribution by random measurements
  Assume a uniform distribution over the observable range as the distribution in case of a random observation. The maximum value of the sensor is simulated as z_{max}.

$$p_{rand}(z_t|x_t, m) = \begin{cases} \frac{1}{z_{max}} & \text{if } 0 \leq z_t < z_{max} \\ 0 & \text{otherwise} \end{cases} \tag{4}$$

In this study, an observation model using beacons was constructed by combining these weighted models. The model was constructed by adding these weights, where $w_{hit} + w_{rand} = 1$.

$$p(z_t|x_t, m) = w_{hit} \cdot p_{hit} + w_{rand} \cdot p_{rand} \tag{5}$$

C. Use of ceiling reflection

As an algorithm that also utilizes the reflected path of the ceiling of a beacon, we used a virtual beacon that is specularly reflected by the ceiling, as shown in Fig. 1. Because there are two possible coordinates for one environmental beacon (real coordinates and specular reflection coordinates), the coordinates to be adopted were determined using maximum likelihood estimation based on the likelihood calculated by the observation model in the previous section. This algorithm is shown in Algorithm 1.

First, we compute the ①direct distance $z^{*,d}_t$ from the beacon on the map to the position of the particle, and the ②reflection path distance $z^{*,r}_t$ obtained from the position m_r of the virtual beacon specularly reflected on the ceiling. For each of these distances $(z^{*,d}_t, z^{*,r}_t)$ calculated from the map, the actual observed value z_t is placed into the beam model to obtain the likelihood. Finally, the likelihoods obtained by the ① direct distance and the ② reflection path are compared, and a larger likelihood is adopted.

D. Use of reflective pathways other than ceilings

In reality, the measured distance may not be the ceiling reflection path at the time of the NLoS, and a large error due to unexpected reflections may be added. Even so, because the reflected path is measured, **the measured distance is greater than the actual direct distance from the environmental beacon to the robot.** As a result, even if measurements are obtained as a result of unexpected reflections, this property can be used to loosely constrain the robot.

When using the observation model (Algorithm 1), an exception was made when the direct path calculated from all

Algorithm 1 Observation model

Require: z_t: Measuring distance
Require: $x_t := (x, y, \theta)$: State of one particle
Require: $m := (m_x, m_y, m_z)$: Environment side beacon coordinates
Require: h_r: Height of robot side beacon
Require: h_c: Ceiling height
Ensure: w_t: Particle weight

function MEASUREMENT$(z_t, x_t, m, h_r, h_c, w_t)$
    $z_t^{*,d} \leftarrow |x_t - m|$
    $w_t^d \leftarrow z_{hit} \cdot \mathcal{N}(z_t; z_t^{d,*}, \sigma_{hit}^2)$
    if $z_t < z_{max}$ **then**
        $w_t^d \leftarrow w_t^d + z_{rand} \cdot \frac{1}{z_{max}}$
    end if
    $m^r \leftarrow (m_x, m_y, h_c + (h_c - m_z))$
    $z_t^{*,r} \leftarrow |x_t - m^{*,r}|$
    $w_t^r \leftarrow z_{hit} \cdot \mathcal{N}(z_t; z_t^{*,r}, \sigma_{hit}^2)$
    if $z_t < z_{max}$ **then**
        $w_t^r \leftarrow w_t^r + z_{rand} \cdot \frac{1}{z_{max}}$
    end if
    $w_t \leftarrow \max(w_t^d, w_t^r)$
    return w_t
end function

particles in the current particle distribution $\mathcal{X}_t$, the predicted ceiling reflection values $z_t^{*,d}, z_t^{*,r}$ is evidently far from the observation z_t.

$$\forall x_t \in \mathcal{X}_t, |z_t - z_t^{*,d}(x_t)| > \sigma_{th} \land |z_t - z_t^{*,r}(x_t)| > \sigma_{th} \quad (6)$$

In real-world experiments, when the distance between the observation and $\sigma_{th} = 1.5[m]$ or more, the observation is not weighted by the observation model (Algorithm 1) because it is considered that the observation is not caused by a direct path or ceiling reflection path. Instead, at least the true posture is considered to be inside the measurement distance. We set the weights of particles outside the measurement distance to zero, and loosely constrained the weights of particles inside to be normalized.

VI. EXPERIMENTS

The robot equipped with the beacon navigated manually along the path shown in Fig. 4a in two real environments: one with obstacles in front of the beacon (①) and one with dynamic obstacles (②). The data logs of various sensors were obtained by manually running the robot along the path shown in Fig. 4a. In this experiments, the visual odometry using a 6D SLAM module (SiNGRAY AExlam80/T, HMS) is used.

The results for these two environments are shown in Figs. 5-7 depicts how the direct path/ceiling reflection path is discriminated for each particle during the observation update. It can be observed that the particle distribution improved with the addition of the beacon. Even when only the ceiling reflection path is available in the environment because of an obstacle (desk) (Fig.7a), the ceiling reflection path is

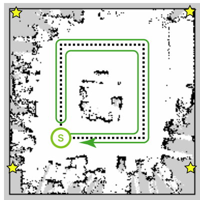

(a) **Environmental map.** Beacons are placed at a height of 1.8 m in the four corners of the room (marked with a star). The beacons are mounted on the robot at a height of 0.5 m. The robot manually runs counterclockwise and clockwise from the starting point in the lower left corner while collecting measurement data.

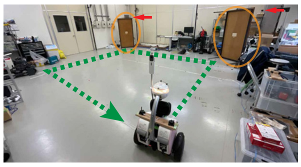

(b) ①**Obstacles.** Obstacles (1.8-meter-high desks marked with orange circles) are placed in front of transmission beacons (red arrows).

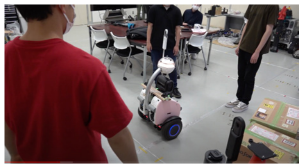

(c) ②**People around the robot.** Two people walk in front of the robot, while one walks behind it.

Fig. 4: **Experimental setup**

correctly identified and used. Even in an environment with dynamic obstacles and unstable beacon-based distance measurement, the measured distance can be seen to differentiate between the direct path, ceiling reflection path, and others.

A motion-capture camera was also installed in the environment to verify the accuracy of the estimation. There were eight motion capture cameras installed at a height of approximately 2.5 meters. We set up a 2 m x 2 m rectangle as the robot's running path, which was used to measure motion capture.

Five estimation methods were compared: combining LiDAR(Section V-A), beacon (V-B), reflection (V-C), and outlier methods (V-D). As in the previous experiment, the robot was manually driven in two real environments: one with obstacles in front of the beacon, and the other with people around it.

The resulting positions obtained from the motion capture camera were used as the ground truth, and the average error for each combination of methods is shown in Table I. Error transitions are shown in Fig. 8, and the respective estimations are shown in Figs. 9-10.

As a result, the estimation method combining all methods (v) shows the highest performance when obstacles are present. On the other hand, in the case where people walk around the robot, estimation methods (iv) and (v) show the highest performance, with similar values.

In contrast, estimation methods (ii) and (iii), which do not consider outliers, exhibit large positioning errors. In these methods, once a large measurement is taken for some reason, such as multiple reflections, the estimated position becomes inaccurate and varies significantly. Note that in these experiments, when the outlier model was selected, the rejection of loose constraints did not work effectively because all particles were within the measured distance in most cases.

These results suggest that the estimation method that includes reflection paths is effective for estimating NLoS signals caused by large obstacles, whereas the outlier method may be effective for estimating NLoS signals caused by people in the environment who appear suddenly.

The current method only considers ceiling reflections and treats other reflections as outliers. Future work will include the addition of other reflections, such as from walls and floors, to make the method more accurate and robust. The effectiveness of the loosely constrain in the outlier model will also be further investigated.

VII. CONCLUSIONS

In this study, we propose a position estimation method that combines a wireless range sensor and 2D-LiDAR. In particular, to solve the NLoS problem of wireless range sensors, which occurs in the presence of dynamic obstacles, we propose a method that utilizes reflections from the ceiling by arranging the sensors in an ingenious manner. We will continue to conduct experiments in real environments to develop an indoor location-estimation method that can deal with dynamic obstacles.

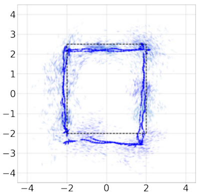

(a) 2D-LiDAR only

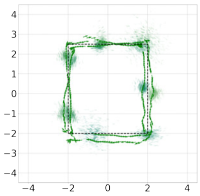

(b) Proposed method (2D-LiDAR + beacon)

Fig. 5: ①**Results when obstacles exist.** Estimated positions and particle distributions are measured at regular time intervals.

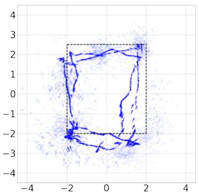

(a) 2D-LiDAR only

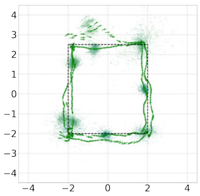

(b) Proposed method (2D-LiDAR + beacon)

Fig. 6: ②**Result when people walk around the robot.** Estimated positions and particle distributions are measured at regular time intervals. Two people walked in front of the robot and one walked behind it. A 2D-LiDAR measures 180° in front of the robot.

ACKNOWLEDGMENT

This work was partially supported by JST, the establishment of university fellowships towards the creation of science technology innovation, Grant Number JPMJFS2132, and the Cabinet Office (CAO), Cross-ministerial Strategic Innovation Promotion Program (SIP), "An intelligent knowledge processing infrastructure, integrating physical and virtual domains" (funding agency: NEDO).

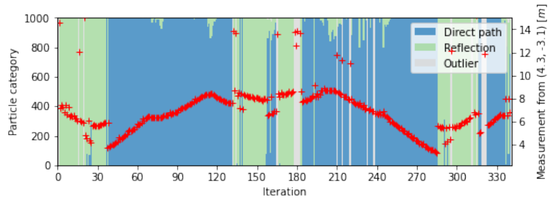

(a) ①**Results when obstacles exist.**

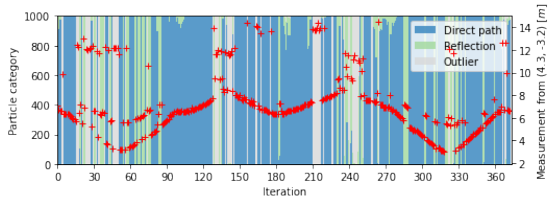

(b) ②**Result when people walk around the robot.**

Fig. 7: **Categories of particles estimating the direct path or ceiling reflection.** Categories of particles for the beacon are in the lower right corner of the map. The horizontal axis represents the number of updates. (Left vertical axis) Blue: The number of particles used to estimate the direct path, Green: ceiling reflection, White: The number of particles whose predicted and measured values differ by more than σ_{th}. Total number of particles is 1000. (Right vertical axis) Red: Distance measured by the beacon is in the lower right corner of the map.

REFERENCES

[1] Y. Song *et al.*, "UWB/LiDAR Fusion For Cooperative Range-Only SLAM," in *2019 International Conference on Robotics and Automation (ICRA)*, vol. 2019-May. IEEE, may 2019, pp. 6568–6574. [Online]. Available: http://arxiv.org/abs/1811.02854 https://ieeexplore.ieee.org/document/8794222/

[2] W. Zhen and S. Scherer, "Estimating the Localizability in Tunnel-like Environments using LiDAR and UWB," in *2019 International Conference on Robotics and Automation (ICRA)*, vol. 2019-May. IEEE, may 2019, pp. 4903–4908. [Online]. Available: https://ieeexplore.ieee.org/document/8794167/

[3] J. Khodjaev *et al.*, "Survey of NLOS identification and error mitigation problems in UWB-based positioning algorithms for dense environments," *annals of telecommunications - annales des télécommunications*, vol. 65, no. 5-6, pp. 301–311, jun 2010. [Online]. Available: http://link.springer.com/10.1007/s12243-009-0124-z

[4] E. Dijk, K. van Berkel, R. Aarts, and E. van Loenen, "Ultrasonic 3d position estimation using a single base station," in *Ambient Intelligence*, E. Aarts, R. W. Collier, E. van Loenen, and B. de Ruyter, Eds. Berlin, Heidelberg: Springer Berlin Heidelberg, 2003, pp. 133–148.

[5] K.-W. Kim, J. Kwon, C.-G. Lee, and J. Han, "Accurate indoor location tracking exploiting ultrasonic reflections," *IEEE Sensors Journal*, vol. 16, no. 24, pp. 9075–9088, 2016.

[6] "Marvelmind robotics," https://marvelmind.com/, accessed: 2022-07-01.

[7] S. Thrun *et al.*, *Probabilistic Robotics (Intelligent Robotics and Autonomous Agents)*. The MIT Press, 2005.

[8] S. Macenski *et al.*, "The marathon 2: A navigation system," in *2020 IEEE/RSJ International Conference on Intelligent Robots and Systems (IROS)*, 2020, pp. 2718–2725.

	(i) LiDAR	(ii) LiDAR +Beacon	(iii) LiDAR +Beacon +Reflection	(iv) LiDAR +Beacon +Outlier	(v) LiDAR +Beacon +Reflection +Outlier
1. Obstacles	0.250	0.818	2.864	0.294	0.137
2. People around the robot	0.311	0.971	2.032	0.162	0.160

TABLE I: **Mean Position Estimation Error [m].** In methods (ii) and (iii), tracking is significantly off from the middle of the operation, and the values are larger.

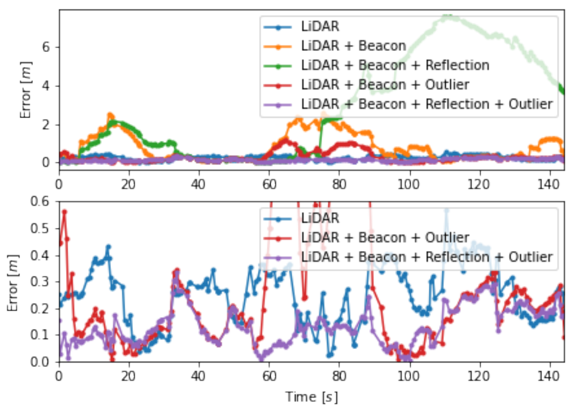

(a) ①**Error when obstacles exist.**

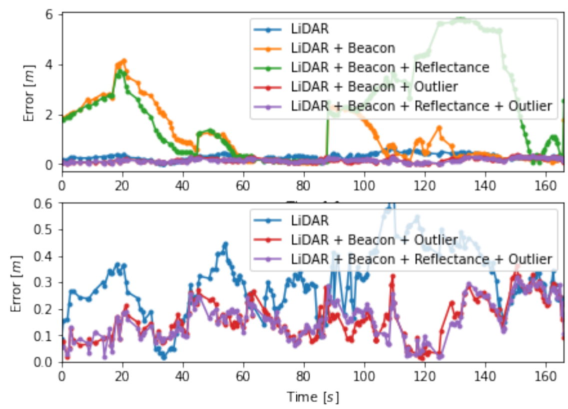

(b) ②**Error when people walk around the robot.**

Fig. 8: **Error per time.** Only the Y-axis scale differs between the upper and lower figures.

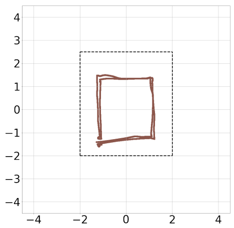

(a) Ground truth (VICON)

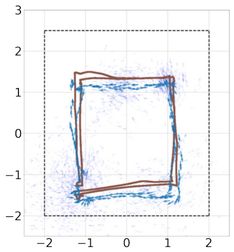

(b) 2D-LiDAR

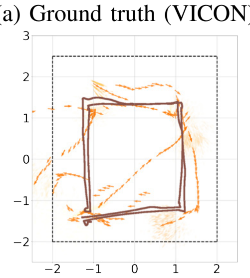

(c) 2D-LiDAR + Beacon

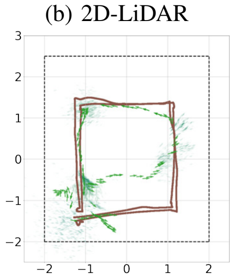

(d) 2D-LiDAR + Beacon + Reflection

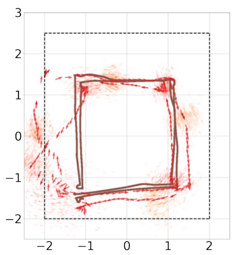

(e) 2D-LiDAR + Beacon + Outlier

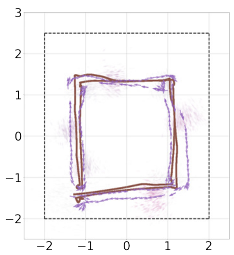

(f) 2D-LiDAR + Beacon + Reflection + Outlier

Fig. 9: ①**Result when obstacles exist.** Estimated positions and particle distributions are measured at regular time intervals.

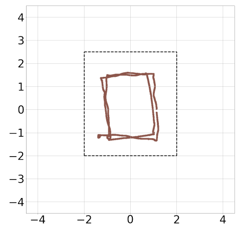

(a) Ground truth (VICON)

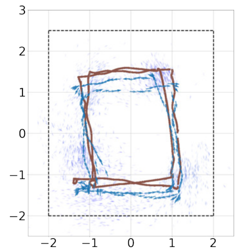

(b) 2D-LiDAR

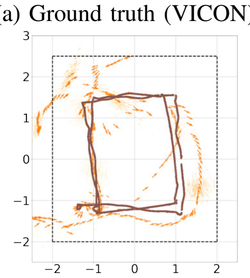

(c) 2D-LiDAR + Beacon

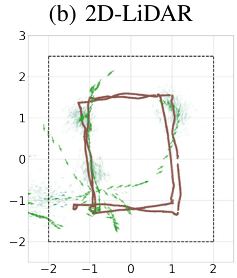

(d) 2D-LiDAR + Beacon + Reflection

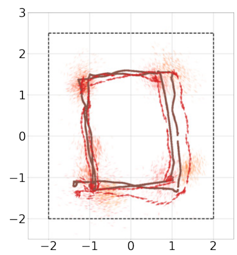

(e) 2D-LiDAR + Beacon + Outlier

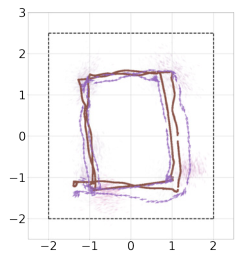

(f) 2D-LiDAR + Beacon + Reflection + Outlier

Fig. 10: ②**Result when people walk around the robot.** Estimated positions and particle distributions are measured at regular time intervals.